Second amorphous-to-crystalline phase transformation in $Cu_{60}Ti_{20}Zr_{20}$ bulk metallic glass

2007 J. Phys.: Condens. Matter 19 246206

(http://iopscience.iop.org/0953-8984/19/24/246206)

J. Phys.: Condens. Matter **19** (2007) 246206 (10pp) doi:10.1088/0953-8984/19/24/246206

Second amorphous-to-crystalline phase transformation in $Cu_{60}Ti_{20}Zr_{20}$ bulk metallic glass

Q P Cao[1,2], J F Li[1,4], P N Zhang[1], A Horsewell[3], J Z Jiang[2] and Y H Zhou[1]

[1] State Key Laboratory of Metal Matrix Composites, School of Materials Science and Engineering, Shanghai Jiao Tong University, Shanghai 200030, People's Republic of China
[2] Laboratory of New-Structured Materials, Department of Materials Science and Engineering, Zhejiang University, Hangzhou 310027, People's Republic of China
[3] Department of Manufacturing Engineering and Management, Building 204, Technical University of Denmark, DK-2800 Lyngby, Denmark

E-mail: jfli@sjtu.edu.cn

Received 27 December 2006, in final form 10 April 2007
Published 18 May 2007
Online at stacks.iop.org/JPhysCM/19/246206

Abstract

The second amorphous-to-crystalline phase transformation in $Cu_{60}Ti_{20}Zr_{20}$ bulk metallic glass was investigated by differential scanning calorimetry and x-ray diffractometry. The difference of the Gibbs free energies between the amorphous phase and the crystalline products during the transformation is estimated to be about 2.46 kJ mol^{-1} at 753 K, much smaller than the 61 kJ mol^{-1} obtained assuming that it is a polymorphic transformation. It was revealed that the phase transformation occurs through a eutectic crystallization of $Cu_{51}Zr_{14}$ and Cu_2TiZr, having an effective activation energy of the order of 400 kJ mol^{-1}. The average Avrami exponent n is about 2.0, indicating that the crystallization is diffusion controlled.

1. Introduction

Due to lack of long-range translational order in the atomic assembly, bulk metallic glasses (BMGs) exhibit many unique properties, such as excellent corrosion resistance, good magnetic property, remarkably high strength and hardness, and large elastic deformation limit [1–4], which allow them to be a class of potential engineering materials for structural and functional applications. The high elastic limit of 2% strain is of major interest for many structural applications, but BMGs show insignificant macroscopic plasticity at room temperature and fail by fracture when solicited beyond their elastic limit [5]. One possible way to overcome this shortfall is to prepare intrinsic BMG nanocomposites by controlled partial crystallization of the BMG matrix [6, 7]. Therefore, careful studies of the nanocrystallization process are of great significance. The crystallization kinetics of BMGs has been a main issue because

[4] Author to whom any correspondence should be addressed.

of the practical and theoretical interest in crystal nucleation and growth in high undercooling conditions.

Recently, the ternary Cu–Ti–Zr alloys with more than 50 at.% copper, excellent glass-forming ability (GFA) and novel mechanical properties have attracted considerable research work [8–20]. One of them is $Cu_{60}Ti_{20}Zr_{20}$, with a near-eutectic composition. It crystallizes in the supercooled liquid region through two exothermic reactions corresponding to the amorphous-to-$Cu_{51}Zr_{14}$ phase transformation and the residual amorphous phase transformation [9, 16, 17, 19]. Although a polymorphous crystallization for the residual amorphous phase transformation in $Cu_{60}Ti_{20}Zr_{20}$ glass was proposed [16], sufficient evidence was not presented to support this argument. The mechanism of the residual amorphous phase transformation is still unclear; therefore, in the present work a detailed investigation of the residual amorphous phase transformation in $Cu_{60}Ti_{20}Zr_{20}$ BMG was performed.

2. Experimental details

Alloy ingots with the nominal composition of $Cu_{60}Ti_{20}Zr_{20}$ (at.%) were prepared by arc melting mixtures of Cu (99.99 wt%), Zr (99.9 wt%) and Ti (99.9 wt%) in a purified argon atmosphere. Cylindrical $Cu_{60}Ti_{20}Zr_{20}$ rods of 2 mm diameter were prepared by copper mould suction casting. The amorphous nature of the as-cast specimens was verified by x-ray diffraction (XRD) using a Philips PW1820 x-ray diffractometer with monochromatic Cu Kα radiation and transmission electron microscopy (TEM) using a JEOL JEM-3000F instrument operating at 300 kV. Thermal analyses were performed in a Pyris Diamond power compensation differential scanning calorimeter (DSC) under a flow of purified argon at a heating rate of 20 K min^{-1}. The specimen and reference pans were made of aluminium. The temperature and the heat flow were calibrated by measuring the melting temperatures and the heats of fusion of pure In, Sn and Zn. The melting behaviour of the specimen was analysed on a Netzsch DSC 404 C under a continuous argon flow at a heating rate of 10 K min^{-1}.

To study the isothermal transformation of the residual amorphous phase, the amorphous specimen was heated to 766 K at 20 K min^{-1} in a DSC instrument in order to complete the first exothermic reaction, and then immediately cooled down to room temperature at 200 K min^{-1} to get the 'starting material'. In subsequent isothermal treatment of the residual amorphous phase, the 'starting material' was heated to the isothermal temperatures at 20 K min^{-1} and held isothermally.

3. Results and discussion

Figure 1 shows the DSC curves of the as-cast and pre-annealed $Cu_{60}Ti_{20}Zr_{20}$ specimens. The as-cast specimen exhibits an endothermic event, characterized by a glass transition temperature $T_g = 706$ K, followed by two exothermic events, characterized by the onset temperature of crystallization $T_x = 736$ K, the peak temperature of the first crystallization event $T_{p1} = 748$ K and the peak temperature of the second crystallization event $T_{p2} = 786$ K. The enthalpies of the first exothermic event ΔH_1 and of the second exothermic event ΔH_2 are 19 and 28 J g^{-1}, respectively. The melting behaviour of the $Cu_{60}Ti_{20}Zr_{20}$ specimen is shown in figure 2. The melting temperature T_m and liquid temperature T_l are determined to be 1100 and 1132 K, respectively. The reduced glass transition temperature $T_{rg}(T_{rg} = T_g/T_l)$ [21] and γ value ($\gamma = T_x/(T_g + T_l)$) [22], which are critical parameters in expressing the GFA of an alloy, are 0.624 and 0.400, respectively. To investigate the crystallization products of the second exotherm, four specimens were heated at 20 K min^{-1} to 766, 786, 813 and 850 K, respectively, and then cooled down to ambient temperature at 200 K min^{-1}. The corresponding XRD patterns are

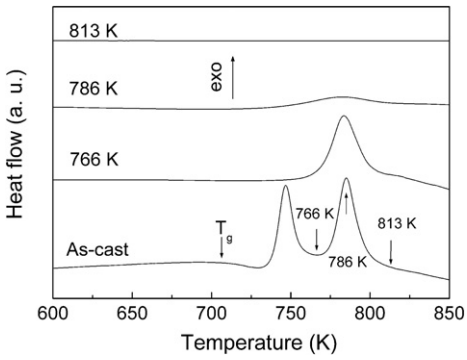

Figure 1. DSC curves for as-cast $Cu_{60}Ti_{20}Zr_{20}$ BMG and the specimens isochronally pre-annealed to different temperatures, at a heating rate of 20 K min^{-1}.

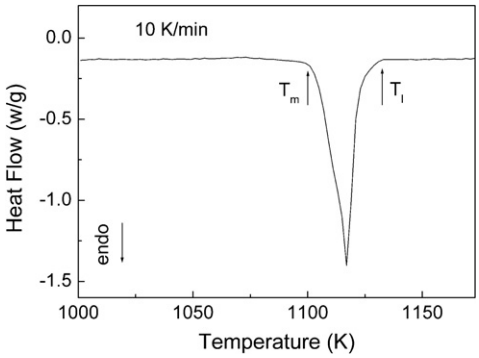

Figure 2. Melting behaviour of the as-cast $Cu_{60}Ti_{20}Zr_{20}$ BMG at a heating rate of 10 K min^{-1}.

shown in figure 3. The specimen heated up to 766 K exhibits a broad amorphous hump similar to the as-cast specimen, and no diffraction peaks from crystalline phases are detected. The origin of undetectable crystalline peaks in this annealed specimen has already been revealed to be overlapping of the diffraction peaks of $Cu_{51}Zr_{14}$ phase with small crystallite sizes [17]. The specimens isochronally heated to 786, 813 and 850 K show evidence for crystallization with an enhancement of the crystalline component in the XRD patterns at the expense of the amorphous component. The diffraction peaks of the specimen isochronally heated to 850 K can be indexed to hexagonal $Cu_{51}Zr_{14}$ and hexagonal Cu_2TiZr, while the diffraction patterns of the specimen isochronally heated to 813 K are dominated by the diffraction peaks of $Cu_{51}Zr_{14}$ phase but the diffraction peaks of Cu_2TiZr phase are very weak, indicating that the grain growth of Cu_2TiZr phase is very slow during the residual amorphous phase transformation. It should be noted that the intensities of the diffraction peaks of hexagonal $Cu_{51}Zr_{14}$ recorded from the specimen pre-annealed up to 813 K were much stronger than that pre-annealed to 766 K. In the case of the residual amorphous phase transformation, two possible crystallization mechanisms should be taken into account. The first one is that Cu_2TiZr phase forms through a polymorphous reaction of the residual amorphous phase and the increased intensity of the diffraction peaks of hexagonal $Cu_{51}Zr_{14}$ is caused by the grain coalescence, and the second one is that this transformation occurs through a eutectic crystallization reaction between $Cu_{51}Zr_{14}$ and Cu_2TiZr phases, which involves the atomic diffusion and partitioning of solute.

To further study the residual amorphous phase transformation, isothermal measurement at different temperatures was performed. Figure 4 depicts the isothermal DSC thermograms of the residual amorphous phase transformation at 743, 748, 753, 758 and 763 K, where the specimens have been pre-annealed through the first crystallization reaction before the isothermal treatment. Isochronal DSC scans up to 850 K were performed immediately

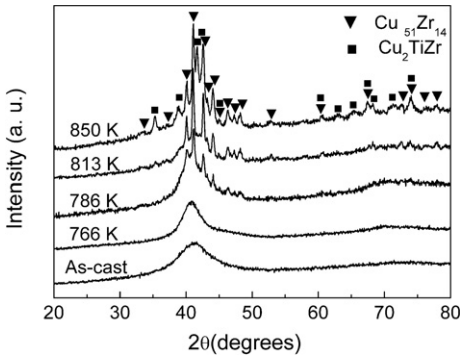

Figure 3. XRD patterns recorded for the as-cast $Cu_{60}Ti_{20}Zr_{20}$ BMG and specimens isochronally annealed to different temperatures.

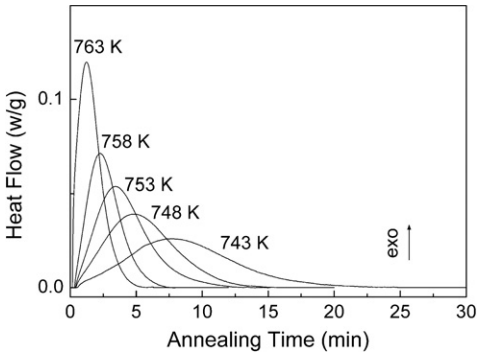

Figure 4. Isothermal DSC thermograms of the second phase transformation at 743, 748, 753, 758 and 763 K for the $Cu_{60}Ti_{20}Zr_{20}$ specimen that has been isochronally pre-annealed to 766 K at a heating rate of 20 K min^{-1}.

following the isothermal measurements in order to determine whether the specimens had crystallized completely during the isothermal anneals, and it was found that there were no endothermic or exothermic events in all the isochronal scans. All the isothermal DSC traces exhibit only one single exothermic peak after a certain incubation time. The measurement performed at the lowest isothermal temperature of 743 K reveals one sluggish exothermic event whose reaction time reaches approximately 25 min. As the annealing temperature increases up to 763 K, the crystallization time decreases to 5 min. The incubation time, τ, prior to crystallization is 0.15, 0.29, 0.35, 0.44 and 0.56 min at the annealing temperature of 763, 758, 753, 748 and 743 K, respectively. It is well known that time–temperature-transformation (TTT) curves for crystallization of the amorphous material usually possess a nose or parabolic shape, and the top half of the nose relates to nucleation of crystalline seeds while the lower half to growth of these seeds [23]. In the present work, only the lower part of the TTT curve for the residual amorphous phase transformation is observed, indicating that the crystallization is mainly growth dominated. A possible reason could be that the $Cu_{51}Zr_{14}$ nanocrystals with an average size of about 7 nm embedded in the residual amorphous matrix having undergone the first crystallization reaction can act as nuclei for the residual amorphous phase transformation [19], and the growth process occurs directly in these sites.

The Arrhenius plot of the incubation time, τ, as a function of temperature for the residual amorphous phase transformation in the $Cu_{60}Ti_{20}Zr_{20}$ BMG is shown in figure 5 according to the following equation:

$$\tau = \tau_0 \exp(E_n/RT) \tag{1}$$

where E_n is an activation energy for nucleation, τ_0 a constant, R the gas constant and T the isothermal temperature. E_n can be evaluated from the slope of the linear fit of the data.

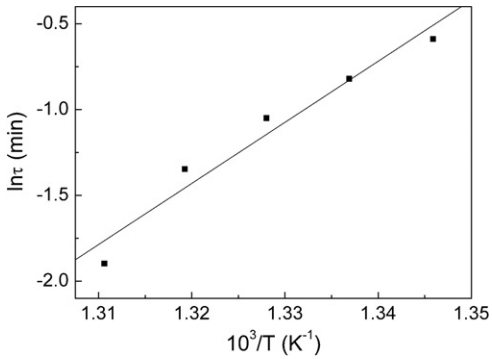

Figure 5. The Arrhenius plot of the incubation time directly from the experiment as a function of temperature for the residual amorphous phase transformation of the $Cu_{60}Ti_{20}Zr_{20}$ BMG.

The activation energy of nucleation for the residual amorphous phase transformation in the $Cu_{60}Ti_{20}Zr_{20}$ BMG is found to be 300 ± 35 kJ mol^{-1}.

Crystallization of amorphous alloys proceeds via nucleation and growth. The kinetics of such a transformation is often described in terms of Johnson–Mehl–Avrami (JMA) theory [24–27]. Due to homogeneous distribution of primary $Cu_{51}Zr_{14}$ phase after the first crystallization reaction in the $Cu_{60}Ti_{20}Zr_{20}$ BMG, the residual amorphous phase transformation through heterogeneous nucleation at the pre-existing primary particles still can be described by the phenomenological JMA model. When the heat release measured in figure 4 is assumed to be proportional to the crystallized volume fraction, the relative volume fraction of the crystalline phase as a function of time can be deduced. The time evolution of the volume fraction of a phase can be described as

$$x(t) = 1 - \exp\{-[k(t-\tau)]^n\} \tag{2}$$

where $x(t)$ is the volume fraction of the transformed phase, t the annealing time, n a constant related to the mechanism of nucleation and growth and k a kinetic constant of the process expressed by the Arrhenius equation $k = k_0 \exp(-E_a/RT)$, where k_0 is a pre-exponential factor and E_a is crystallization activation energy. Equation (2) can also be rewritten as follows:

$$\ln[-\ln(1-x)] = n \ln k + n \ln(t-\tau). \tag{3}$$

The JMA plots of $\ln[-\ln(1-x)]$ against $\ln(t-\tau)$ for limited experimental data ($0.2 \leqslant x \leqslant 0.8$) at different temperatures are shown in figure 6. The rate constant k and the Avrami exponent n can be calculated from the intercept and slope of the linear fitting to the JMA plot. Figure 7 shows the plots of $\ln k$ versus $1/T$, and the effective activation energy for the residual amorphous phase transformation in the $Cu_{60}Ti_{20}Zr_{20}$ BMG was found to be 398 ± 18 kJ mol^{-1}. The value for the effective activation energy is in good agreement with the value of 347 ± 29 kJ mol^{-1}, deduced from Kissinger plots for an as-spun $Cu_{60}Ti_{20}Zr_{20}$ ribbon [19]. If the residual amorphous phase transformation occurs through a polymorphous reaction, no long-range atomic diffusion is required for the transformation, and the effective activated energy should be a small value. In most polymorphous crystallization processes, the effective activation energy ranges from 100 to 220 kJ mol^{-1} depending upon the amorphous alloy system [28, 29]. Moreover, the Avrami exponent n with an average value of 2.0 is much lower than the typical value of 3–4 for polymorphous phase transformation with the interface-controlled crystallization mechanism [30]. This indicates that the residual amorphous phase

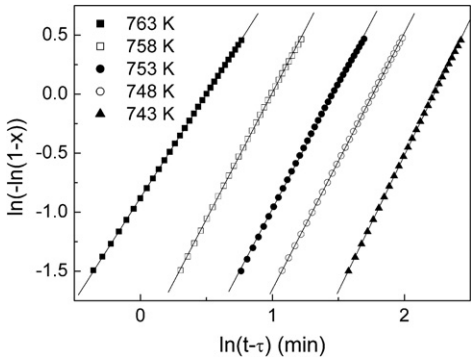

Figure 6. The JMA plots of $\ln[-\ln(1-x)]$ versus $\ln(t-\tau)$ for limited experimental data ($0.2 \leqslant x \leqslant 0.8$) at different temperatures for the residual amorphous phase transformation of the $Cu_{60}Ti_{20}Zr_{20}$ BMG.

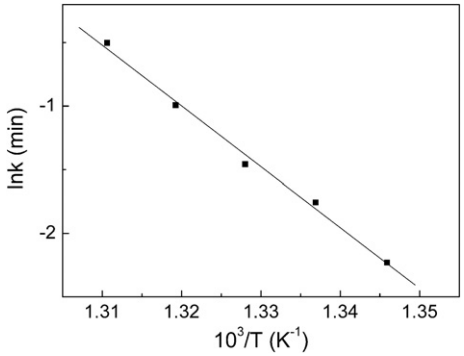

Figure 7. Arrhenius plot of effective rate constant, k, as a function of temperature for the residual amorphous phase transformation in the $Cu_{60}Ti_{20}Zr_{20}$ BMG, in which k is obtained from JMA plots as listed in table 1.

transformation may be a eutectic reaction with a diffusion-controlled process in $Cu_{60}Ti_{20}Zr_{20}$ BMG, rather than a polymorphous crystallization. It is clear that the average Avrami exponent n at different isothermal temperatures is about 2.0, corresponding to three-dimensional diffusion-controlled growth of nuclei at a decreasing nucleation rate according to the classical nucleation theory. For the diffusion-controlled process, $n = 2.5$ corresponds to a steady nucleation rate during phase transformation and $n = 1.5$ zero nucleation rate, while $1.5 < n < 2.5$ corresponds to a decreasing nucleation rate. The larger the value of n in the range of 1.5–2.5, the less remarkable the drop of nucleation rate during transformation. The Avrami exponent n for the residual amorphous phase transformation actually decreases from 2.3 to 1.8 when the isothermal temperature increases from 743 to 763 K. The rise of the isothermal temperature results in the increase of nucleation rate, and the number of nuclei forming in the early stage of phase transformation correspondingly increases. Correspondingly, the number of nuclei forming in the late stage decreases as compared with that at a lower isothermal temperature. Therefore, the decrease of nucleation rate during the isothermal annealing becomes more evident at high temperatures.

The relative volume fraction of a phase during the residual amorphous phase transformation in the $Cu_{60}Ti_{20}Zr_{20}$ BMG as a function of time can be described as $x(t) =$

$1 - \exp[-Y(t)]$, where the expressions of $Y(t)$ for the steady-state and time-dependent nucleation and growth models are given as follows [31].

(1) Heterogeneous nucleation with three-dimensional constant growth rate:

$$Y(t) = \tfrac{4}{3}N\pi u^3 t^3,$$

where N is the nuclei number per unit volume, u is the growth rate, and t is the annealing time.

(2) Heterogeneous nucleation with constant grain size:

$$Y(t) = NV_0,$$

where V_0 is the grain size.

(3) Steady-state nucleation with three-dimensional constant growth rate:

$$Y(t) = \int_0^t I_{\mathrm{st}} \tfrac{4}{3}\pi u^3 (t-x)^3 \,\mathrm{d}x = \tfrac{1}{3}\pi I_{\mathrm{st}} u^3 t^4,$$

where I_{st} is the steady-state nucleation rate.

(4) Steady-state nucleation with constant grain size:

$$Y(t) = \int_0^t I_{\mathrm{st}} V_0 \,\mathrm{d}x = I_{\mathrm{st}} V_0 t.$$

(5) Time-dependent Zeldovich's nucleation with three-dimensional constant growth rate:

$$Y(t) = \int_0^t I(x)\tfrac{4}{3}\pi u^3 (t-x)^3 \,\mathrm{d}x = \tfrac{4}{3}\pi I_{\mathrm{st}-Z} u^3 \int_0^t \exp(-\tau_Z/x)(t-x)^3 \,\mathrm{d}x,$$

where τ_Z and $I_{\mathrm{st}-Z}$ are the incubation time and the steady-state nucleation rate for the Zeldovich's nucleation, respectively.

(6) Time-dependent Zeldovich's nucleation with constant grain size:

$$Y(t) = \int_0^t I(x) V_0 \,\mathrm{d}x = I_{\mathrm{st}-Z} V_0 \int_0^t \exp(-\tau_Z/x)\,\mathrm{d}x.$$

(7) Time-dependent Kashchiev's nucleation with three-dimensional constant growth rate:

$$Y(t) = \int_0^t I(x)\tfrac{4}{3}\pi u^3 (t-x)^3 \mathrm{d}x = \tfrac{4}{3}\pi I_{\mathrm{st}-K} u^3 \times \left[\frac{t^4}{4} + 2\sum_{m=1}^{\infty}(-1)^m \int_0^t \exp\left(-\frac{m^2 t}{\tau_K}\right)(t-x)^3 \,\mathrm{d}x\right],$$

where τ_K and $I_{\mathrm{st}-K}$ are the incubation time and the steady-state nucleation rate for the Kashchiev's nucleation, respectively.

(8) Time-dependent Kashchiev's nucleation with constant grain size:

$$Y(t) = \int_0^t I(x) V_0 \,\mathrm{d}x = I_{\mathrm{st}-K} V_0 \left[t + 2\sum_{m=1}^{\infty} \frac{(-1)^m \tau_K [1 - \exp(-m^2 t/\tau_K)]}{m^2}\right].$$

It was found that models 2 and 4 cannot fit the data at all. Models 6 and 8 can fit the data much better than models 1, 3, 5 and 7, which indicates that the crystals rapidly grow and then reach saturation during the process of isothermal treatment. Figure 8 shows the fitting results using the typical models 1, 3, 6 and 8 for the relative crystallized volume fraction with time at 743 K. Figure 9 exemplifies the fitting results using model 8 for the five isothermal annealing temperatures. The deduced parameters using models 6 and 8 are listed in table 1. These results imply the existence of a time-dependent nucleation process for the residual amorphous phase transformation in the $Cu_{60}Ti_{20}Zr_{20}$ BMG.

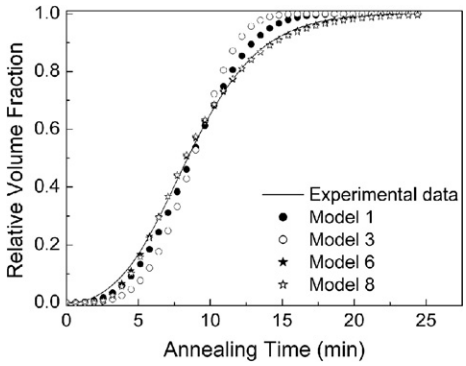

Figure 8. Relative volume fractions of the crystalline component as a function of time at the isothermal annealing temperature of 743 K for the residual amorphous phase transformation in the $Cu_{60}Ti_{20}Zr_{20}$ BMG. The solid line is the experimental data while the points are the fitting results using models 1, 3, 6 and 8.

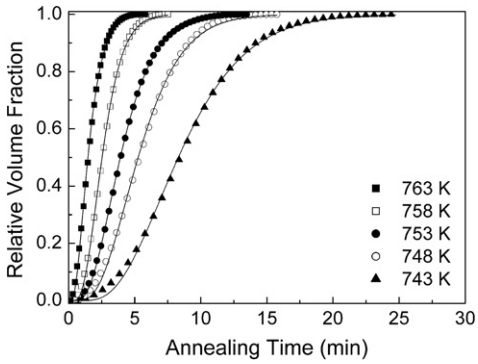

Figure 9. Relative volume fractions of the crystalline component as a function of time at different temperatures for the residual amorphous phase transformation in the $Cu_{60}Ti_{20}Zr_{20}$ BMG. The solid line is the data deduced from figure 4 and the points are the fitting results using model 8.

Table 1. Parameters obtained from the experiment, the JMA model, model 6 and model 8 at five isothermal temperatures for the residual amorphous phase transformation in the $Cu_{60}Ti_{20}Zr_{20}$ BMG.

	Parameters	743 K	748 K	753 K	758 K	763 K
Experimental	τ (min)	0.56 ± 0.02	0.44 ± 0.01	0.35 ± 0.01	0.29 ± 0.01	0.15 ± 0.01
JMA Model	k (min^{-1})	0.107 ± 0.001	0.173 ± 0.001	0.233 ± 0.002	0.371 ± 0.002	0.605 ± 0.005
	n	2.3 ± 0.1	2.2 ± 0.1	2.1 ± 0.2	2.1 ± 0.2	1.8 ± 0.2
Model 6	$I_{st-z}V_0$ (min^{-1})	0.55 ± 0.01	0.80 ± 0.02	0.92 ± 0.02	1.73 ± 0.05	1.67 ± 0.02
	τ_z (min)	8.21 ± 0.03	4.90 ± 0.03	3.22 ± 0.02	2.40 ± 0.03	1.50 ± 0.02
Model 8	$I_{st-k}V_0$ (min^{-1})	0.32 ± 0.03	0.47 ± 0.02	0.56 ± 0.02	1.01 ± 0.03	1.15 ± 0.02
	τ_k (min)	4.70 ± 0.03	2.80 ± 0.02	1.90 ± 0.02	1.41 ± 0.01	0.83 ± 0.01

In the Zeldovich's nucleation and growth model [32], the transient nucleation time, τ_Z, can be expressed as

$$\tau_Z = (256\pi\sigma^6\nu^4)/(9\Delta\mu^6 k^+_{d^*}) \tag{4}$$

where $k^+_{d^*}$ is the rate of monomer addition to a nucleus with size d^*, $\Delta\mu$ is the difference of the Gibbs free energies per molecule between the crystalline and amorphous phases, σ is the

interfacial energy per unit area, and ν is the molecular volume. In the Kashchiev's nucleation and growth model [33], the transient nucleation time, τ_K, can be written as

$$\tau_K = (256 k_B T \sigma^3 \nu^2)/(\pi \Delta\mu^4 k^+_{d^*}) \tag{5}$$

where k_B is the Boltzmann's constant. The ratio of the transient nucleation times in both models is given by $\tau_K/\tau_Z = (9 k_B T \Delta\mu^2)/(\pi^2 \sigma^3 \nu^2)$.

According to the parameters of Cu_2TiZr phase in [34], the difference of the Gibbs free energies per molecule between Cu_2TiZr and the residual amorphous phase is calculated to be about 61 kJ mol^{-1} at 753 K, provided that the residual amorphous phase transformation is a polymorphous reaction. The difference of the Gibbs free energy between the crystals and the residual amorphous phases, $\Delta\mu$, can be determined by using $\tau_K/\tau_Z = (9 k_B T \Delta\mu^2)/(\pi^2 \sigma^3 \nu^2) = 0.59$ at $T = 753$ K. The molecular volume of the residual amorphous phase is roughly substituted by $\nu = 8.8$ cm^3 mol^{-1} of the $Cu_{60}Ti_{20}Zr_{20}$ glass calculated by the molecular mass and the density from the Archimedean principle. The solid–liquid interfacial energy σ is calculated following the Miedema and Broeder approach [35], and the equation can be written as

$$\sigma = 0.211 d \Delta H_f/\nu + 0.52 \times 10^{-7} T/\nu^{2/3} \tag{6}$$

where ΔH_f is the heat of fusion per molecule, $d = (\nu/N_0)^{1/3}$ and N_0 is Avogadro's constant. For the $Cu_{60}Ti_{20}Zr_{20}$ glass synthesized here, the value of ΔH_f is calculated to be 4.746 kJ mol^{-1} from the high-temperature DSC curve. Assuming that the ratio of the heat of fusion per molecule of the phases formed in the amorphous-to-$Cu_{51}Zr_{14}$ phase transformation to that in the residual amorphous phase transformation is similar to the ratio of the enthalpy per gram of the phases formed in the amorphous-to-$Cu_{51}Zr_{14}$ phase transformation to that in the residual amorphous phase transformation, the heat of fusion per molecule, ΔH_f, of the phases formed in the residual amorphous phase transformation can be determined to be 2.827 kJ mol^{-1}. The solid–liquid interfacial energy σ for the phases formed in the residual amorphous phase transformation is calculated to be 0.108 J m^{-2}. Therefore, the difference of the Gibbs free energy between the crystals and the residual amorphous phases, $\Delta\mu$, is found to be around 2.46 kJ mol^{-1}, which is much smaller than the value of 61 kJ mol^{-1} assuming that the residual amorphous phase transformation is a polymorphous reaction. According to the existing theory for heterogeneous nucleation, the critical energy barrier ΔG_c associated with the formation of a nucleus with the critical size of r_c can be expressed as

$$\Delta G_c = \frac{1}{3}\pi r_c^2 \sigma (2 - 3\cos\alpha + \cos^3\alpha) = \frac{4}{3}\frac{\pi\sigma^3}{\Delta\mu^2}(2 - 3\cos\alpha + \cos^3\alpha) \tag{7}$$

where α is the contact angle between the nucleus and the extrinsic agent. The small value of the Gibbs free energy difference, $\Delta\mu$, between the crystals and the residual amorphous phases is consistent with the high effective activation energy about 400 kJ mol^{-1} for the residual amorphous phase to transform through a eutectic reaction, much larger than the typical value, 100–220 kJ mol^{-1}, of effective activation energy for a polymorphous transition. Thus, it is further confirmed that the residual amorphous phase transformation in $Cu_{60}Ti_{20}Zr_{20}$ glass is a eutectic reaction.

4. Conclusions

It is found that the residual amorphous phase transformation in the $Cu_{60}Ti_{20}Zr_{20}$ glass is a eutectic crystallization reaction of two crystalline phases, $Cu_{51}Zr_{14}$ and Cu_2TiZr phase. The effective activation energy for crystallization, E_a, was found to be about 400 kJ mol^{-1}, and

the average Avrami exponent n is about 2.0, indicating that atomic diffusion may involve the residual amorphous phase transformation and the crystallization process proceeds with a decreasing nucleation rate. The difference of the Gibbs free energy per molecule between the crystals and the residual amorphous phase is estimated to be around 2.46 kJ mol^{-1} at 753 K, which is a much smaller value as compared with 61 kJ mol^{-1} assuming the residual amorphous phase transformation is a polymorphous reaction, leading to a higher value of effective activation energy than the typical value for a polymorphous transition.

Acknowledgments

Financial support from the National Natural Science Foundation of China under grant No 50471016 and the DANIDA Fellowship Centre are gratefully acknowledged. We wish to thank F Faupel and K Ratzke for discussion on activation energy.

References

[1] Greer A L 1995 *Science* **267** 1947
[2] Johnson W L 1999 *MRS Bull.* **24** 42
[3] Inoue A 2000 *Acta Mater.* **48** 279
[4] Wang W H, Dong C and Shek C H 2004 *Mater. Sci. Eng.* R **44** 45
[5] Spaepen F 1977 *Acta Metall.* **25** 407
[6] Lu K 1996 *Mater. Sci. Eng.* R **16** 161
[7] Fan C and Inoue A 2000 *Appl. Phys. Lett.* **77** 46
[8] Inoue A, Zhang W, Zhang T and Kurosaka K 2001 *Mater. Trans.* **42** 1149
[9] Inoue A, Zhang W, Zhang T and Kurosaka K 2001 *Acta Mater.* **49** 2645
[10] Louzguine D V and Inoue A 2002 *J. Mater. Res.* **17** 2112
[11] Kasai M, Saida J, Matsushita M, Ohsuna T, Matsubara E and Inoue A 2002 *J. Phys.: Condens. Matter* **14** 13867
[12] Chen Y T, Zhang T, Zhang W, Ping D H, Hono K, Inoue A and Sakurai T 2002 *Mater. Trans.* **43** 2647
[13] Sordelet D J, Rozhkova E, Huang P, Wheelock P B, Besser M F, Kramer M J, Clavo-Dahlborg M and Dahlborg U 2002 *J. Mater. Res.* **17** 186
[14] Park E S, Lim H K, Kim W T and Kim D H 2002 *J. Non-Cryst. Solids* **298** 15
[15] Jiang J Z, Saida J, Kato H, Ohsuna T and Inoue A 2003 *Appl. Phys. Lett.* **82** 4041
[16] Jiang J Z, Yang B, Saksl K, Franz H and Pryds N 2003 *J. Mater. Res.* **18** 895
[17] Jiang J Z, Kato H, Ohsuna T, Saida J, Inoue A, Saksl K, Franz H and Ståhl K 2003 *Appl. Phys. Lett.* **83** 3299
[18] Calin M, Eckert J and Schultz L 2003 *Scr. Mater.* **48** 653
[19] Concustell A, Revesz A, Surinach S, Baro M D, Varga L K and Heunen G 2004 *J. Mater. Res.* **19** 505
[20] Cao Q P, Li J F, Zhou Y H and Jiang J Z 2003 *J. Phys.: Condens. Matter* **15** 8703
[21] Lu Z P, Li Y and Ng S C 2000 *J. Non-Cryst. Solids* **270** 103
[22] Lu Z P and Liu C T 2003 *Phys. Rev. Lett.* **91** 115505
[23] Lemon G H and Boolchand P 1987 *J. Non-Cryst. Solids* **91** 1
[24] Johnson W A and Mehl R F 1939 *Trans. Am. Inst. Min. Metall. Pet. Eng.* **135** 416
[25] Avrami M 1939 *J. Chem. Phys.* **7** 1103
[26] Avrami M 1940 *J. Chem. Phys.* **8** 212
[27] Avrami M 1941 *J. Chem. Phys.* **9** 177
[28] Ye F and Lu K 1998 *Acta Mater.* **46** 5965
[29] Zhou F, Luck R, Lu K, Lavernia E J and Ruhle M 2002 *Phil. Mag.* A **82** 1003
[30] Christian J W 2002 *The Theory of Transformation in Metals and Alloy* (Oxford: Pergamon)
[31] Jiang J Z, Zhuang Y X, Rasmussen H, Saida J and Inoue A 2001 *Phys. Rev.* B **64** 094208
[32] Zeldovich J B 1943 *Acta Physicochim. URSS* **18** 1
[33] Kashchiev D 1969 *Surf. Sci.* **14** 209
[34] Arroyave R, Eagar T W and Kaufman L 2003 *J. Alloys Compounds* **351** 158
[35] Miedema A R and den Broeder F J A 1979 *Z. Metallkd.* **70** 14